

EVOLUTIONARY MAP OF THE UNIVERSE: DETECTION OF THE WOLF-RAYET STAR WR40

A. C. Bradley¹ , Z. J. Smeaton¹ , M. D. Filipović¹ , N. F. H. Tothill¹ 
R. Z. E. Alsaberi^{2,1} , J. D. Collier^{3,4,1} , Y. A. Gordon⁵ , A. M. Hopkins⁶  and H. Zakir¹ 

¹ Western Sydney University, Locked Bag 1797, Penrith South DC, NSW 2751, Australia

E-mail: 20295208@student.westernsydney.edu.au

² Faculty of Engineering, Gifu University, 1-1 Yanagido, Gifu 501-1193, Japan

³ Australian SKA Regional Centre, Curtin Institute of Radio Astronomy (CIRA),
1 Turner Avenue, Technology Park, Bentley, Western Australia, 6102

⁴ The Inter-University Institute for Data Intensive Astronomy (IDIA), Department of Astronomy,
University of Cape Town, Private Bag X3, Rondebosch, 7701, South Africa

⁵ Department of Physics, University of Wisconsin-Madison, 1150 University Avenue, Madison, WI 53706, USA

⁶ School of Mathematical and Physical Sciences, 12 Wally's Walk, Macquarie University, NSW 2109, Australia

(Received: May 29, 2025; Accepted: August 23, 2025)

SUMMARY: We present a radio-continuum detection of the well-known Wolf-Rayet star WR40 at 943.5 MHz using observations from the Evolutionary Map of the Universe (EMU) survey. We find that the shell surrounding WR40, known as RCW 58, has a flux density of 158.9 ± 15.8 mJy and the star itself is 0.41 ± 0.04 mJy. The shell size is found to be $9' \times 6'$, which matches well with the shell in $H\alpha$ and is similarly matched to the shell at $22 \mu\text{m}$ in infrared. Using *Gaia* data, we derive a linear size of $7.32(\pm 0.34) \times 4.89(\pm 0.23)$ pc at a distance of 2.79 ± 0.13 kpc. We use the previous Australia Telescope Compact Array (ATCA) observations at 8.64, 4.80, and 2.4 GHz to determine a spectral index of WR40, which is estimated to be $\alpha = 0.80 \pm 0.11$, indicating that the emission from the star is thermal.

Key words. Radio continuum: stars – Stars: Wolf-Rayet – ISM: individual objects: WR40 – Astrometry

1. INTRODUCTION

Wolf-Rayet (WR) stars are late-stage stars, and are often defined by their mass loss rate compared to previous evolutionary stages (Nugis and Lamers 2000), creating outbursts of stellar material mainly comprised of the star's dominating element (Marston 1995). They are characterised by the elements dom-

inating their spectra: either carbon, nitrogen, or oxygen (Crowther 2007). The elemental composition of WR stars categorises them into three main types: WC (carbon-rich), WN (nitrogen-rich), and WO (oxygen-rich).

WR40 is a well-known WN8 type WR star (Hamann et al. 2006) accompanied by a shell known as RCW 58, which has also been studied extensively (Hartquist et al. 1986). RCW 58 is unique, possessing a non-uniform, irregular nature, likely caused by interactions of the wind-driven ejecta with the Interstellar Medium (ISM) (Hartquist et al. 1986, Marston 1995, Jiménez-Hernández et al. 2021). WR40 is often

© 2025 The Author(s). Published by Astronomical Observatory of Belgrade and Faculty of Mathematics, University of Belgrade. This open access article is distributed under CC BY-NC-ND 4.0 International licence.

linked to WR16 (Antokhin et al. 1995, Cichowski et al. 2020, Bradley et al. 2025a), another WN8 star. They are similar, but WR40’s shell is quite irregular and elliptical, whereas WR16’s is symmetrical and circular (Marston 1995). WR stars are known to have variability, with WR40 showing significant variability compared to others (Gosset et al. 1989).

The EMU survey (Hopkins et al. 2025, Norris et al. 2011, 2021) is mapping the entire southern sky at 943.5 MHz using the Australian Square Kilometre Array Pathfinder (ASKAP) (Hotan et al. 2021). Owing to the telescope’s high sensitivity, we often detect low-surface brightness features that have not been previously characterized. Some of these objects are Supernova Remnants (SNRs); G305.4-2.2 (Teleios; Filipović et al. 2025b), J0624-6948 (Filipović et al. 2022, Sasaki et al. 2025), G288.8-6.3 (Ancora; Filipović et al. 2023, Burger-Scheidlin et al. 2024), G308.7+1.4 (Raspberry; Lazarević et al. 2024b), G312.6+2.8 (Unicycle; Smeaton et al. 2024); a pulsar wind nebula (PWN) (Potoroo; Lazarević et al. 2024a); a reflection nebula (RNe) (Bradley et al. 2025b); and possible candidates for the source of the Ultra-high-energy Neutrino Event KM3-230213A (Filipović et al. 2025a).

2. DATA

2.1. ASKAP EMU

WR40 and its shell have been seen in two EMU observations. SB46948 observed the tile EMU_1136-64 on December 12 2022, and SB54771 observed the tile EMU_1050-64 on November 11 2023. These observations were reduced using the standard ASKAP pipeline, ASKAPSoft, using multi-frequency synthesis imaging, multi-scale cleaning, self-calibration and convolution to a common beam size (Guzman et al. 2019). We then combined the observations into a single image using the Miriad (Sault et al. 1995) task IMCOMB. The final image was created using equal weighting, resulting in a lower root mean square (RMS) noise level of $\sim 30 \mu\text{Jy beam}^{-1}$. The final image is shown in Fig. 1.

2.2. Other Data

We use values from the *Gaia* Data Release 3 (DR3) catalogue observations (Gaia Collaboration et al. 2016b, 2023) to determine the distance to WR40, as well as determining the true size of the radio shell surrounding it.

We also include observations from the SuperCOSMOS (656.281 nm Hambly et al. 2001) and Wide-field Infrared Survey Explorer (WISE) (22 μm Wright et al. 2010) sky surveys to compare the nebulosity surrounding WR40 at different wavelengths (Fig. 2).

The central star WR40 is seen in RACS-High (1655.5 MHz Hale et al. 2021) as measured in the Sydney Radio Stars Catalogue (Driessen et al. 2024). It is also measured at 943.5 MHz, but because the

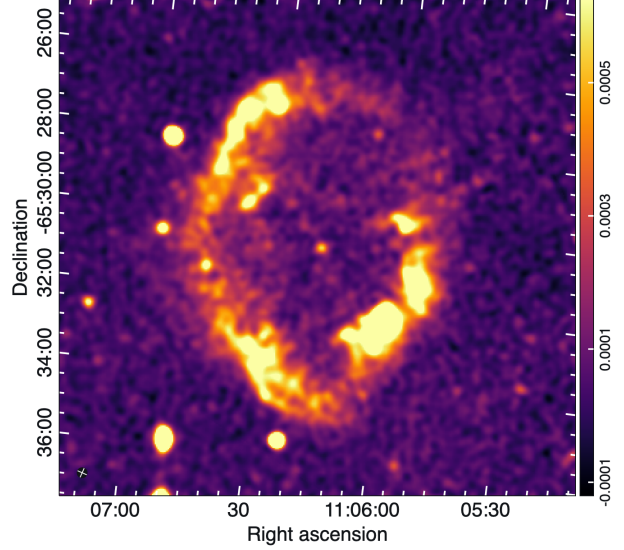


Fig. 1: EMU 943.5 MHz radio-continuum image of WR40 and its surrounding shell RCW 58 at 15'' resolution. Image is linearly scaled.

integrated flux is much higher than our EMU flux, we have elected to use none of the catalogue’s measurements in our analysis.

3. RESULTS AND DISCUSSION

In relation to WR40, there are disparities between parallax values in the previous literature (Perryman et al. 1997, van Leeuwen 2007, Gaia Collaboration et al. 2016a). We use the *Gaia* Data Release 3 (DR3) parallax of 0.3572 ± 0.0170 milliarcseconds (Gaia Collaboration 2020) to estimate a distance for WR40 to be 2.79 ± 0.13 kpc. We use this distance and the angular diameter measured from the EMU image ($9' \times 6'$) to determine the true size of the shell to be $7.32 \pm 0.34 \times 4.89 \pm 0.23$ pc. Within this defined region, we measure the flux density of the WR40 nebulosity to be 158.9 ± 15.8 mJy, taking a 10% error (Filipović et al. 2022, 2024). We also measure WR40 itself and find its flux density to be 0.41 ± 0.04 mJy.

Using the previous ATCA measurements, we can determine a spectral index for the star WR40. Leitherer et al. (1995) determines a flux density of 2.52 ± 0.09 mJy at 8.64 GHz, and 1.69 ± 0.10 mJy at 4.80 GHz. Chapman et al. (1999) measured the star WR40 at 2.40 GHz, estimating a flux density of 1.21 ± 0.13 mJy. The spectral index is defined as $S \propto \nu^\alpha$, where S is flux density, ν is frequency, and α is spectral index (Filipović and Tothill 2021). Using the three ATCA measurements and our EMU measurement, we estimate a spectral index of $\alpha = 0.80 \pm 0.11$, indicating thermal emission from the star. We obtain a consistent measurement using only the 1999 observations, suggesting the radio variability isn’t signifi-

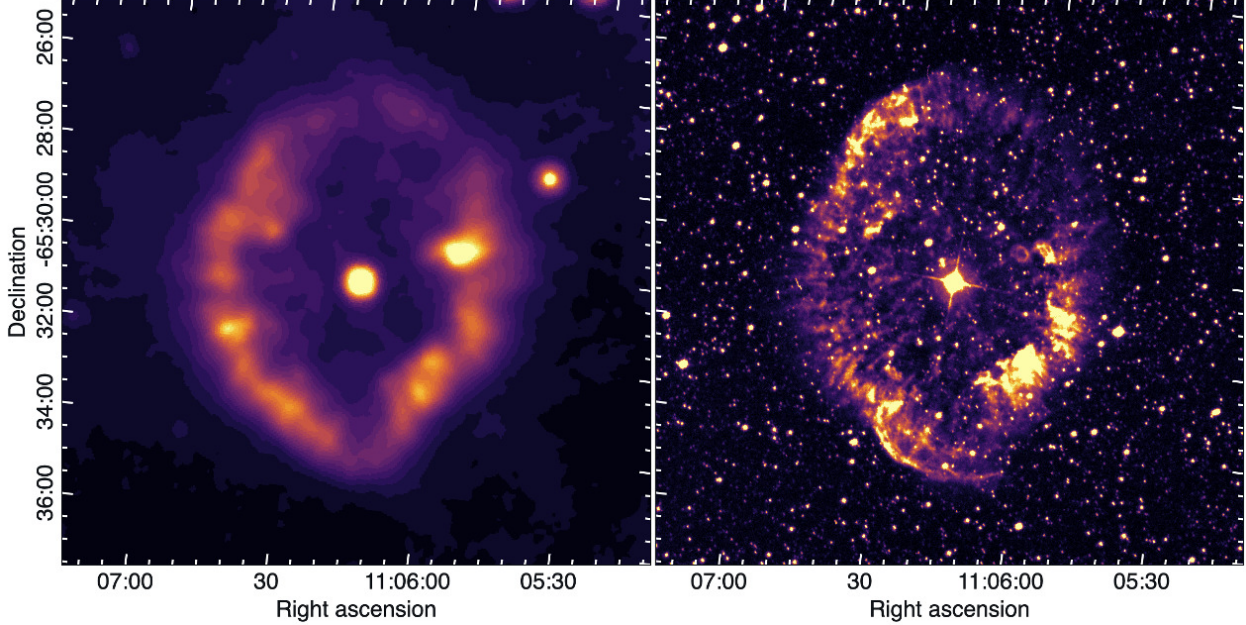


Fig. 2: WR40 and its surrounding shell RCW 58, both images are linearly scaled. – **Left:** WISE infrared image in the W4 band at $22\text{ }\mu\text{m}$. – **Right:** SuperCOSMOS H α (656.281 nm) image.

cantly impacting our spectral index measurement, despite WR40 showing variability at other wavelengths (Gosset et al. 1989).

The emission seen at 943.5 MHz matches well with SuperCOSMOS H α and WISE 22 μm (Fig. 3), which may indicate that the radio emission is thermal. We have attempted to obtain additional radio data in order to constrain the nature of the emission of the shell, by measuring fluxes from the Sydney University Molonglo Sky Survey (SUMSS) (Bock et al. 1999) and Parkes-MIT-NRAO (PMN) survey (Griffith and Wright 1993). We also obtained flux measurements detailed in Jiménez-Hernández et al. (2021) from ATCA observations. However, we were unable to determine a reliable spectral index with any of these observations due to the changes in sensitivity and the low surface brightness of the source.

Prajapati et al. (2019) explored the non-thermal nature of a WO-type WR star with a spectral index of -0.81 ± 0.1 . We have applied this spectral index to our EMU measurement to predict a SUMSS flux at 843 MHz. We predict an expected flux of ~ 173 mJy, as this is brighter than the EMU emission, we would expect a reliable detection. However, WR40 as seen by SUMSS is almost indistinguishable from the background noise. This makes the thermal scenario more likely, however, there is not enough evidence to rule out the non-thermal scenario. It is possible that the follow up observations with a sensitive telescope like MeerKAT (Jonas and MeerKAT Team 2016) could help constrain the nature of the emission.

Marston (1995) shows observations of [O III] which extends outside the radio shell toward the south-east

portion which does not appear in the EMU observation, but is partially seen in the WISE image. Differences in the shell of the three observations may be partially explained by differences in resolution, however there are some noticeable bright spots present in the WISE (Fig. 2, Left) observation that are not present in the EMU and SuperCOSMOS H α observations. Due to the irregular shape of RCW 58, it is likely that the wind from WR40 is expanding into a slower, non-uniform wind from the previous Red Super Giant (RSG), or Luminous Blue Variable (LBV) phase ((Meyer 2021))

4. CONCLUSION

We present a detection of the well known Wolf-Rayet star WR40 and its shell RCW 58 at 43.5 MHz using observations from the EMU survey. The shell as seen by EMU is $9' \times 6'$, and using *Gaia* data, we derive a true size of $7.32(\pm 0.34) \times 4.89(\pm 0.23)$ pc at a distance of 2.79 ± 0.13 kpc. We measure a flux density for RCW 58 to be 158.9 ± 15.8 mJy, and WR40's flux density as 0.41 ± 0.04 mJy. Using the previous ATCA observations, at 8.64, 4.80, and 2.4 GHz, we calculate a spectral index $\alpha = 0.80 \pm 0.11$ for the star WR40 indicating that the emission from the star is thermal. We are unable to determine a spectral index for RCW 58 due to its low surface brightness and inconsistencies in the previous radio observations. Taking observations with telescopes from the latest generation, such as MeerKAT, will help constrain the spectral index and determine the nature of the emission of RCW 58.

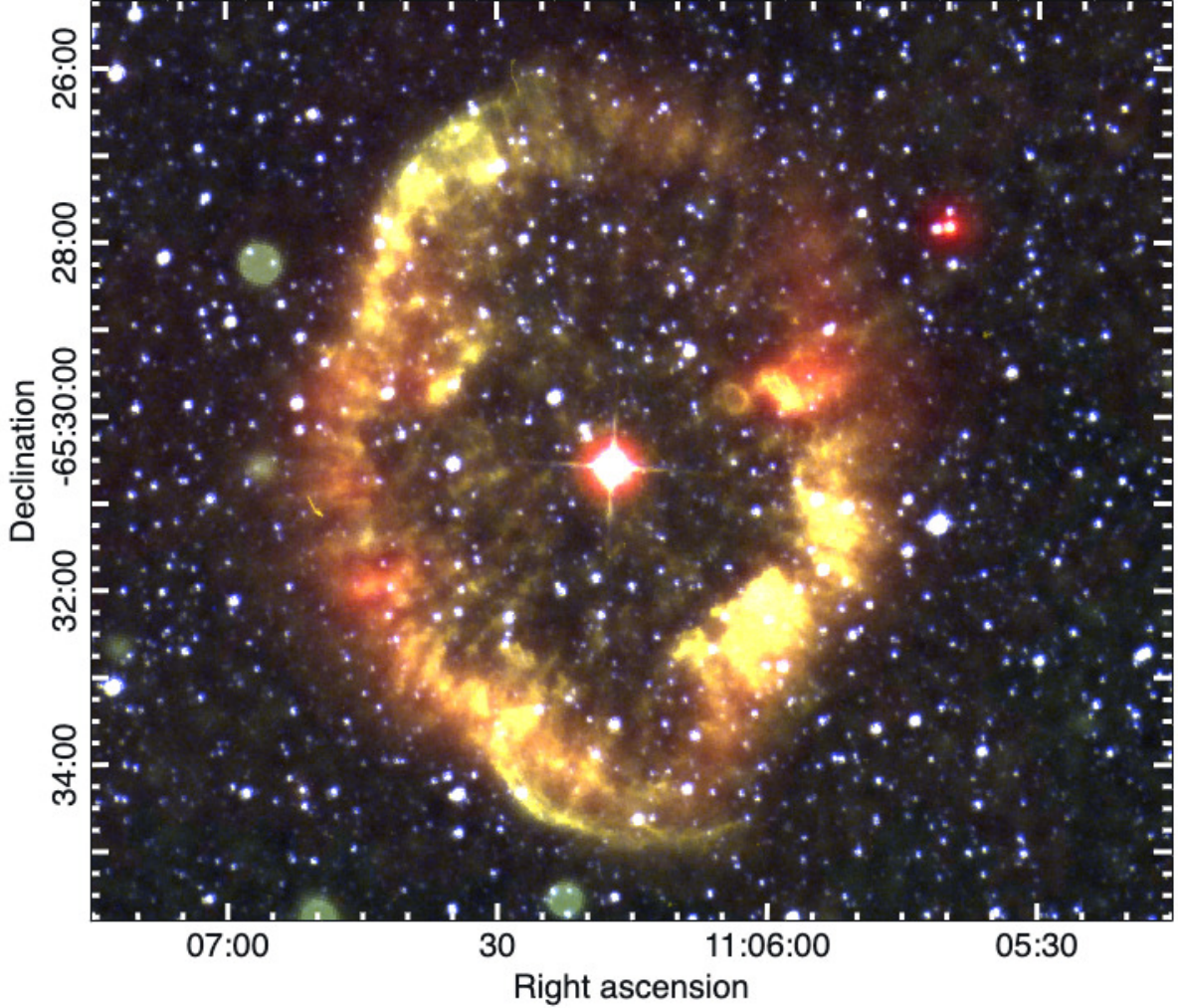


Fig. 3: Four-colour composite image of WR40 and RCW 58. Red is WISE 22 μm , yellow is SuperCOSMOS H α , green is the EMU observation, and blue is the DSS2 red plate provided from Lasker *et al.* (1996).

Acknowledgements – We thank Bärbel S. Koribalski for helpful discussions. This scientific work uses data obtained from Inyarrimanha Ilgari Bundara, the CSIRO Murchison Radio-astronomy Observatory. We acknowledge the Wajarri Yamaji People as the Traditional Owners and native title holders of the Observatory site. CSIRO’s ASKAP radio telescope is part of the Australia Telescope National Facility (<https://ror.org/05qajvd42>). Operation of ASKAP is funded by the Australian Government with support from the National Collaborative Research Infrastructure Strategy. ASKAP uses the resources of the Pawsey Supercomputing Research Centre. Establishment of ASKAP, Inyarrimanha Ilgari Bundara, the CSIRO Murchison Radio-astronomy Observatory and the Pawsey Supercomputing Research Centre are initiatives of the Australian Government, with support from the Government of Western Australia and the Science and In-

dustry Endowment Fund. This work has made use of data from the European Space Agency (ESA) mission *Gaia* (<https://www.cosmos.esa.int/gaia>), processed by the *Gaia* Data Processing and Analysis Consortium (DPAC, <https://www.cosmos.esa.int/web/gaia/dpac/consortium>). Funding for the DPAC has been provided by national institutions, in particular the institutions participating in the *Gaia* Multilateral Agreement.

REFERENCES

Antokhin, I., Bertrand, J.-F., Lamontagne, R., Moffat, A. F. J. and Matthews, J. 1995, *AJ*, **109**, 817
 Bock, D. C. -J., Large, M. I. and Sadler, E. M. 1999, *AJ*, **117**, 1578
 Bradley, A., Filipović, M. D., Smeaton, Z., *et al.* 2025a, *PASA*, **42**, e101
 Bradley, A., Smeaton, Z., Tothill, N., *et al.* 2025b, *PASA*, **42**, 32

Burger-Scheidlin, C., Brose, R., Mackey, J., et al. 2024, *A&A*, **684**, A150

Chapman, J. M., Leitherer, C., Koribalski, B., Bouter, R. and Storey, M. 1999, *ApJ*, **518**, 890

Cichowski, S., Duronea, N. U., Suad, L. A., et al. 2020, *MNRAS*, **495**, 417

Crowther, P. A. 2007, *ARA&A*, **45**, 177

Driessen, L. N., Pritchard, J., Murphy, T., et al. 2024, *PASA*, **41**, e084

Filipović, M. D. and Tothill, N. F. H. 2021, Principles of Multimessenger Astronomy (IOP Publishing)

Filipović, M. D., Payne, J. L., Alsaberi, R. Z. E., et al. 2022, *MNRAS*, **512**, 265

Filipović, M. D., Dai, S., Arbutina, B., et al. 2023, *AJ*, **166**, 149

Filipović, M. D., Lazarević, S., Araya, M., et al. 2024, *PASA*, **41**, e112

Filipović, M. D., Smeaton, Z. J., Bradley, A. C., et al. 2025a, *ApJL*, **984**, L52

Filipović, M. D., Smeaton, Z. J., Kothes, R., et al. 2025b, *PASA*, **42**, e104

Gaia Collaboration. 2020, *VizieR Online Data Catalog: Gaia EDR3* (Gaia Collaboration, 2020), VizieR Online Data Catalog: I/350. Originally published in: 2021A&A...649A...1G

Gaia Collaboration, Brown, A. G. A., Vallenari, A., et al. 2016a, *A&A*, **595**, A2

Gaia Collaboration, Prusti, T., de Bruijne, J. H. J., et al. 2016b, *A&A*, **595**, A1

Gaia Collaboration, Vallenari, A., Brown, A. G. A., et al. 2023, *A&A*, **674**, A1

Gosset, E., Vreux, J. M., Manfroid, J., et al. 1989, *MNRAS*, **238**, 97

Griffith, M. R. and Wright, A. E. 1993, *AJ*, **105**, 1666

Guzman, J., Whiting, M., Voronkov, M., et al. 2019, *ASKAPsoft: ASKAP science data processor software*, Astrophysics Source Code Library, record ascl:1912.003

Hale, C. L., McConnell, D., Thomson, A. J. M., et al. 2021, *PASA*, **38**, e058

Hamann, W. -R., Gräfener, G. and Liermann, A. 2006, *A&A*, **457**, 1015

Hambly, N. C., MacGillivray, H. T., Read, M. A., et al. 2001, *MNRAS*, **326**, 1279

Hartquist, T. W., Dyson, J. E., Pettini, M. and Smith, L. J. 1986, *MNRAS*, **221**, 715

Hopkins, A., Kapinska, A., Marvil, J., et al. 2025, *PASA*, **42**, e071

Hotan, A. W., Bunton, J. D., Chippendale, A. P., et al. 2021, *PASA*, **38**, e009

Jiménez-Hernández, P., Arthur, S. J., Toalá, J. A. and Marston, A. P. 2021, *MNRAS*, **507**, 3030

Jonas, J. and MeerKAT Team. 2016, in MeerKAT Science: On the Pathway to the SKA, 1

Lasker, B. M., Doggett, J., McLean, B., et al. 1996, in Astronomical Society of the Pacific Conference Series, Vol. 101, Astronomical Data Analysis Software and Systems V, ed. G. H. Jacoby and J. Barnes, 88

Lazarević, S., Filipović, M. D., Dai, S., et al. 2024a, *PASA*, **41**, e032

Lazarević, S., Filipović, M. D., Koribalski, B. S., et al. 2024b, *Research Notes of the American Astronomical Society*, **8**, 107

Leitherer, C., Chapman, J. M. and Koribalski, B. 1995, *ApJ*, **450**, 289

Marston, A. P. 1995, *AJ*, **109**, 1839

Meyer, D. M. -A. 2021, *MNRAS*, **507**, 4697

Norris, R. P., Hopkins, A. M., Afonso, J., et al. 2011, *PASA*, **28**, 215

Norris, R. P., Marvil, J., Collier, J. D., et al. 2021, *PASA*, **38**, e046

Nugis, T. and Lamers, H. J. G. L. M. 2000, *A&A*, **360**, 227

Perryman, M. A. C., Lindegren, L., Kovalevsky, J., et al. 1997, *A&A*, **323**, L49

Prajapati, P., Tej, A., del Palacio, S., et al. 2019, *ApJL*, **884**, L49

Sasaki, M., Zangrandi, F., Filipović, M., et al. 2025, *A&A*, **693**, L15

Sault, R. J., Teuben, P. J. and Wright, M. C. H. 1995, in Astronomical Society of the Pacific Conference Series, Vol. 77, Astronomical Data Analysis Software and Systems IV, ed. R. A. Shaw, H. E. Payne, and J. J. E. Hayes, 433

Smeaton, Z. J., Filipović, M. D., Koribalski, B. S., et al. 2024, *Research Notes of the American Astronomical Society*, **8**, 158

van Leeuwen, F. 2007, *A&A*, **474**, 653

Wright, E. L., Eisenhardt, P. R. M., Mainzer, A. K., et al. 2010, *AJ*, **140**, 1868

**ЕВОЛУЦИОНА МАПА УНИВЕРЗУМА:
ДЕТЕКЦИЈА ВОЛФ-РАЈЕТОВЕ ЗВЕЗДЕ WR40**

A. C. Bradley¹ , Z. J. Smeaton¹ , M. D. Филиповић¹ , N. F. H. Tothill¹ ,
R. Z. E. Alsaberi^{2,1} , J. D. Collier^{3,4,1} , Y. A. Gordon⁵ , A. M. Hopkins⁶  and H. Zakir¹ 

¹ *Western Sydney University, Locked Bag 1797, Penrith South DC, NSW 2751, Australia*

E-mail: 20295208@student.westernsydney.edu.au

² *Faculty of Engineering, Gifu University, 1-1 Yanagido, Gifu 501-1193, Japan*

³ *Australian SKA Regional Centre, Curtin Institute of Radio Astronomy (CIRA),
1 Turner Avenue, Technology Park, Bentley, Western Australia, 6102*

⁴ *The Inter-University Institute for Data Intensive Astronomy (IDIA), Department of Astronomy,
University of Cape Town, Private Bag X3, Rondebosch, 7701, South Africa*

⁵ *Department of Physics, University of Wisconsin-Madison, 1150 University Avenue, Madison, WI 53706, USA*

⁶ *School of Mathematical and Physical Sciences, 12 Wally's Walk, Macquarie University, NSW 2109, Australia*

УДК 523.38 : 52–421.4 : 52–58

Оригинални научни рад

Представљамо прву детекцију познате Волф-Рајет звезде из наше галаксије WR40 у радио-континууму на 943.5 MHz користећи ЕМУ (Еволуциона Мапа Универзума) преглед неба. Нашли смо да љуска која окружује WR40, такође позната и као RCW 58, има густину флукса од 158.9 ± 15.8 mJy за разлику од саме звезде чија је густина флукса 0.41 ± 0.04 mJy. Величина саме љуске је процењена на $9' \times 6'$, што је слично оптичким и инфрацрвеним (на 22 μm) мерењима. Користећи податке са *Gaia* сателита и раније проце-

њену даљину од 2.79 ± 0.13 kpc до саме звезде, израчунали смо да је линеарна величина љуске $7.32 (\pm 0.34) \times 4.89 (\pm 0.23)$ pc. Такође смо користили и претходна радио-континуум посматрања са Аустралијског компактног низа телескопа (енг. ATCA) на фреквенцијама од 8.64, 4.80, и 2.4 GHz, а све да би прецизније проценили радио-спектрални индекс, за који смо добили вредност од $\alpha = 0.80 \pm 0.11$ која указује да је емисија која потиче са саме Волф-Рајет звезде термалног порекла.